Palaeogeography, Palaeoclimatology, Palaeoecology 414 (2014) 260–272

Contents lists available at ScienceDirect

Palaeogeography, Palaeoclimatology, Palaeoecology

journal homepage: www.elsevier.com/locate/palaeo

High resolution climate and environmental changes of the northern Japan (East) Sea for the last 40 kyr inferred from sedimentary geochemical and pollen data

Sergey A. Gorbarenko [a,*], Seung-Il Nam [b], Yulia V. Rybiakova [a], Xuefa Shi [c], Yanguang Liu [c], Alexander A. Bosin [a]

[a] V.I. Il'ichev Pacific Oceanological Institute, FEB RAS, 43 Baltyiskaya Str., Vladivostok, Russia
[b] Korea Polar Research Institute, Songdomirae-ro, Yeonsu-gu, 406-840 Incheon, South Korea
[c] First Institute of Oceanography, State Oceanic Administration, 6 Xianxialing Road, Qingdao 266061, China

ARTICLE INFO

Article history:
Received 5 February 2014
Received in revised form 20 August 2014
Accepted 4 September 2014
Available online 16 September 2014

Keywords:
Northern Japan (East) Sea
Millennial climate changes
Sea level
Last 40 ka

ABSTRACT

High-resolution lithological and isotope-geochemical analyses were made on a well age constrained sediment from the northeastern Japan (East) Sea which recorded 10 dark layers (DL) over the last 40 ka BP. Pollen analysis of the core allows us to reconstruct the history of surrounding landmass vegetation and to determine pronounced vegetation/climate changes. We found that DL 10 which correlated with a DO/Chinese interstadial 8 was forced by increased East Asian humidity and influx of the nutrient-rich water into the sea. DL 5 formed during the cold Heinrich event 3 (HE), at 30–31 ka BP, was most likely to be initiated by the global sea level descent and reduction of seawater exchange with the North Pacific. High resolution of $\delta^{18}O_{pf}$ records reflects a unique sensitivity of the Japan (East) Sea to input of the North Pacific water through the shallow Tsushima and Tsugaru Straits. This led us to the important evidence of the eustatic-sea level changes during the last 40 ka BP. Since 29 ka BP, $\delta^{18}O_{pf}$ curve shows a continuous descending sea level interrupted by sharp drops of HE 2 with a following rise of DO interstadial 2. A sharp $\delta^{18}O_{pf}$ increase since 18.6 ka BP is consistent with coral results which indicate abrupt termination of LGM low stand by a rapid sea level rise initiated at 19.0 ka BP.

1. Introduction

The Japan (East) Sea has experienced dramatic changes in oceanographic conditions during the Late Quaternary in association with both the orbital and suborbital climatic forcing and glacio-eustatic sea level changes (e.g., Oba et al., 1991; Tada et al., 1992, 1999; Gorbarenko and Southon, 2000; Yokoyama et al., 2007). The past oceanographic responses of this marginal sea to the global climate changes and sea level variability are unique because of the shallow Tsushima and Tsugaru Straits with −130 m sills (Fig. 1). Both straits have played a key role in controlling the water exchange between the Japan (East) Sea and the North Pacific.

Gorbarenko (1983, 1993) and Oba et al. (1991, 1995) demonstrated that during the last glacial maximum (LGM) of the Marine Isotope Stage (MIS) 2, $\delta^{18}O$ of planktonic foraminifera ($\delta^{18}O_{pf}$) showed a strong negative excursion implying that there was a distinct decrease in surface water salinity. Because the Japan (East) Sea is connected to the North Pacific through the shallow Tsushima and Tsugaru Straits, a drastic decrease in inflow of the saline Tsushima Warm Current to the marginal sea and prevalence of precipitation above evaporation during the LGM resulted in strong freshening of the surface water (Gorbarenko, 1983; Oba et al., 1991, 1995; Matsui et al., 1998; Gorbarenko and Southon, 2000). The low salinity of the surface water has strengthened the water column stratification, which in turn has drastically decreased the deep water ventilation, leading to euxinic bottom water conditions. As a result, the thin laminated dark sediments with slightly enriched organic carbon contents were deposited during the LGM with a distinct negative excursion in $\delta^{18}O_{pf}$ values (Oba et al., 1991; Gorbarenko and Southon, 2000). A euxinic bottom water condition during the formation of these layers leads to well preserved and abundantly accumulated planktonic foraminiferal tests and barren of the benthic foraminifera (Oba et al., 1991; Gorbarenko and Southon, 2000).

Even though the millennial scale climate changes, such as Dansgaard–Oeschger (DO) events, have been observed first in $\delta^{18}O$ record of Greenland ice core (Dansgaard et al., 1993), many subsequent studies reported DO-like events in other parts of the Earth, including the North Atlantic Ocean, the Japan (East) Sea, and the continental records of East Asia (Tada et al., 1992; 1999; Bond et al., 1997; Wang et al., 2001; Voelker and workshop participants, 2002; Yokoyama et al., 2006). Investigating the linkage of DO oscillations in Greenland and the North Atlantic with those of the distant regions, such as the Japan (East) Sea and its past oceanographic variability is crucial for understanding the driving mechanisms of the global and regional abrupt climate changes during the Late Quaternary. Characteristically, hemipelagic sediments deposited during the Late Quaternary in the

* Corresponding author. Tel.: +7 4232312382; fax: +7 4232312573.
E-mail address: gorbarenko@poi.dvo.ru (S.A. Gorbarenko).

http://dx.doi.org/10.1016/j.palaeo.2014.09.001
0031-0182/

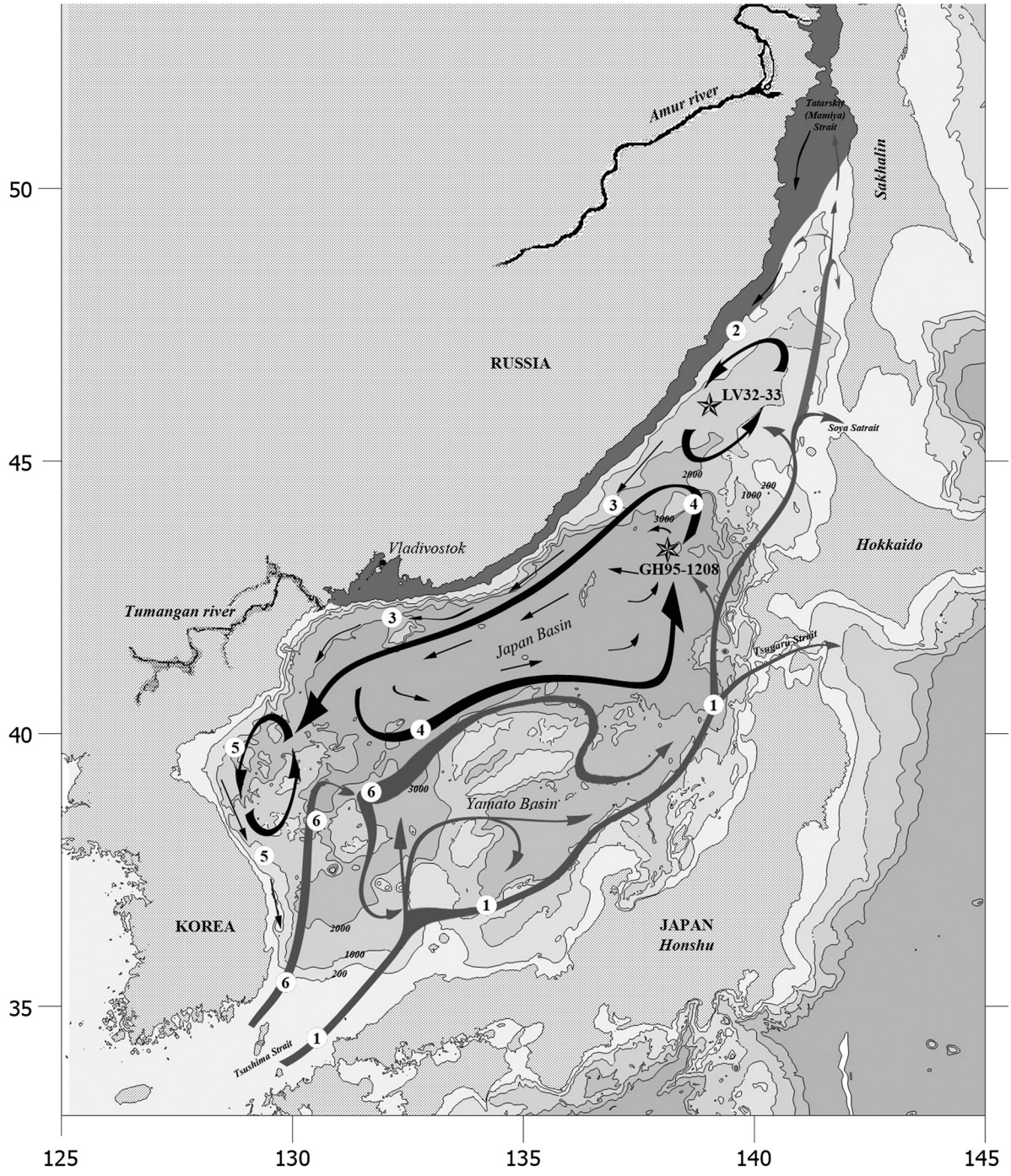

Fig. 1. The bathymetric map of the Japan (East) Sea showing the location of sediment core LV32–33 and core GH95–1208 (Ikehara and Itaki, 2007). The main surface water currents are shown according to Yarichin (1980); 1—Tsushima Warm Current, 2—Shrenk Current, 3—Primorskoye (Liman) Current, 4—South Primorskoye Current, 5—North Korean Cold Current, 6—East Korean Warm Current. Four shallow straits existed around the Japan Sea, namely, Tsushima, Tsugaru, Soya and Tatarskiy Straits. The water depths are ca. 135 m for both Tsushima and Tsugaru Straits and 55 m and 15 m for the Soya and Tatarskiy Straits respectively.

Japan (East) Sea contains centimeter–decimeter scale alternations of organic carbon-rich, thinly laminated dark layers (DL) and organic carbon-poor, homogenous/bioturbated light layers (Tada et al., 1992, 1999). Furthermore, a basin-wide occurrence of alternating dark and light layers shows a synchronicity between southern, central and northeastern parts of the Japan (East) Sea (Oba et al., 1991; Tada et al., 1992; Ikehara, 2003; Itaki et al., 2004; Watanabe et al., 2007; Yokoyama et al., 2007). According to age models of sediment cores from ODP Site 797, cores KH-79-3 and C-3 (Tada et al., 1999), every dark layer above the Aso-4 ash with age of 88 ka BP has been numbered continuously from DL 1 to DL 21 in ascending order from the surface. According to Tada et al. (1999), each dark layer corresponds to DO interstadial (Dansgaard et al., 1993), except for MIS 2 when the sea level was below ca. −90 m (1st Mode of the vertical circulation in the Japan (East) Sea). Because of eustatic sea level changes from −90 m to −60 m (2nd Mode of the vertical circulation) and from −60 m to −20 m (3rd Mode) during the late glacial periods the bottom water condition oscillated from the oxic to suboxic–euxinic conditions (Tada et al., 1999; Yokoyama and Esat, 2011).

The former condition was responsible for sedimentation of thin light layers, whereas the latter one was favorable for the preservation of dark layers with high content of TOC due to an increased inflow of low

salinity from the East China Sea Coastal Water (ECSCW) with high content of nutrients (Tada et al., 1999). According to Tada et al. (1999), the increased inflows of the ECSCW were mainly attributed to the increased precipitation in central and eastern Asia and related enhanced fresh nutrient-rich water discharges from Huanghe and Changjiang rivers to the western Pacific during the warm DO interstadials.

Although Tada et al. (1999) explained the formation of alternating dark and light sediment layers in the Japan (East) Sea, several important questions, particularly, their formation and correlation between organic-rich dark layers and DO cycles, still remain unanswered. For instance, based on the investigation of millennial-scale environmental and sedimentation changes in the Japan (East) Sea for the last 40 ka BP, Itaki et al. (2004) and Yokoyama et al. (2007) have reported significantly different numbers of DL layers, and its age compared to those of Tada et al. (1999). Therefore, the following two task need to be clarified: (1) numbering of major and minor DL layers and finding their correlation with DO cycles in Greenland ice core (NGRIP members, 2004), Chinese Interstadial (CIS) in the Chine cave stalagmite records (Wang et al., 2001; Wang et al., 2008) and Heinrich event (HE) in the North Atlantic (Heinrich, 1988), and (2) transition of DL layers originated from the 1st Mode of the Japan (East) Sea hydrology to the 2nd Mode that is associated with the climate and sea level changes and variability of the ECSCW inflow, respectively. Moreover, the millennial scale environmental and climatic changes in the Japan (East) Sea, the accumulation of alternating dark and light sediment layers, and the associated surrounding landmasses vegetation/climate changes (Yokoyama et al., 2006) are not fully studied and thus insufficient to establish their correlations firmly with DO and Chinese cycles.

In this study, we present high-resolution, lithological, isotopic and micropaleontological data of a well age constrained sediment core LV 32–33, raised from the northern Japan (East) Sea. The lithological characteristics including color along with records of selected productivity proxies allow us to identify several DL layers for the last 40 ka BP (Fig. 2). High frequent sampling (1–2 cm) of studied core with high sedimentation rate (on average 20 cm/kyr) allows us to reconstruct high resolution of environmental changes in the Japan (East) Sea with a time span of 50–100 years. We also reconstructed millennial scale vegetation associated with climate changes in the surrounding landmasses of Northeastern Asia with the data of pollen spectrum of the studied core (with time resolution of 250–500 years). Finally, we correlated our dated multiproxy records and previously identified DLs in other cores to test the origin of DL layers in the Japan (East) Sea and its linkage with DO and China cycles, aiming to better understand the linkages between the marine environment, DL layer formation and surrounding terrestrial climate changes during the last 40 ka BP.

2. Oceanographic setting of the Japan (East) Sea

The Japan (East) Sea is a semi-enclosed marginal sea located between East Asia and the Japanese Island. The Japan (East) Sea is connected with the East China Sea, the NW Pacific Ocean and the Okhotsk Sea through four shallow straits (Fig. 1). Among them, the southwestern Tsushima Strait and the northeastern Tsugaru Strait are the two deepest straits with sill depths of ~130 m.

At present, the Tsushima Warm Current, a branch of the Kuroshio Current, flows into the Japan (East) Sea through the Tsushima Strait and flows out mainly through the Tsugaru Strait (Fig. 1). The North Korea Cold Current (NKCC), a branch of the Liman Current from the Sea of Okhotsk merged with the returning branch of the TWC, flows southward along the eastern part of the East/Japan Sea. The NKCC meets the northward flowing East Korean Warm Current, a branch of the TWC, at latitude 40° N. A polar front at about 40° N acts as the boundary between two surface water masses with a clear contrast in temperature. We raised a sediment core LV 32–33 in the northern part of the Japan (East) Sea where the southward flowing Liman Cold Current dominates the water column characteristics (Yarichin, 1980; Yoon and Kim, 2009) (Fig. 1).

At present, the intermediate and deep waters of the Japan (East) Sea, formed in the northern part of the basin during winter (Martin et al., 1992) facilitate good ventilation in deeper parts of the water column. The water mass below 200–300 m is called the Japan Sea Proper Water, which is characterized by low temperature (0.1–0.3 °C), low salinity (34.0‰–34.1‰), and high oxygen content (5–6 mL/L) (Gamo et al., 1986; Gydrometeorologiya and gydrochimija morej, 2003). Substantial amount of the East China Sea Coastal Water (ECSCW) and the Yellow Sea waters is transported through TWC into the Japan (East) Sea (Suk et al., 1996) (Fig. 1). The core investigated is located in the northern part of the Japan (East) Sea, a region weakly influenced by the sea ice formation during winter seasons (Yakynin, 1979).

3. Materials and methods

The sediment core LV 32–33 was recovered in the northern Japan (East) Sea (46° 28.8′N, 139° 0.3E′) at water depth of 1140 m during RV "Academician M.A. Lavrent'ev" cruise 32, in 2003 (Fig. 1). Hemipelagic sediments of the studied core are characterized by alternation of dark layers and homogenous/bioturbated light layers. Three thinly laminated dark layers were documented in the middle part of core (212–391, 407–417 and 485–512 cm, Fig. 2).

The planktonic foraminifera, *Neogloboquadrina pachyderma* (sin.) were picked out from >125 μm fraction of sediments and measured for oxygen ($\delta^{18}O$) and carbon ($\delta^{13}C$) isotopes in the Leibniz Laboratory of Kiel University. Sample preparation and analytical procedures were described in Kiefer et al. (2001). Planktonic foraminifera *N. pachyderma* (sin) from fraction 125–250 μm were also picked for AMS ^{14}C dating. The radiocarbon age has been measured by the Leibniz-Laboratory for Radiometric Dating and Isotope Research at Kiel University (Kiel, Germany) and the National Ocean Science Accelerator Mass Spectrometry Facility at Woods Hole Oceanographic Institute (Woods Hole, USA), respectively. All radiocarbon ages were converted into calibrated 2-sigma calendar age ranges using the calibration program CALIB REV 7.0.1 (Stuiver and Reimer, 1993) with the Marine 13 calibration curve (Reimer et al., 2013) (Table 1). We accepted the constant reservoir age of the Japan (East) Sea surface water to be equal to modern value of 400 years (Yokoyama et al., 2007) throughout the studied time period, although this value, could have increased during the glacial and weaker deglacial ventilation (Matsumoto and Yokoyama, 2013).

Sediment for pollen analysis was prepared with the standard method of Grichuk (Sladkov, 1967). Fossil pollen species assemblages were identified using microscope MICMED-1 with magnification of 63–1350 power. For the entire core, 122 sediment samples with 5–10 cm intervals were analyzed for pollen. In most samples, 150 to 840 pollen grains were counted; with intervals 50, 60, 280–310, 615, 620, 760 and 765 cm range within 110–150 grains. In general, pollen grains were more abundant in the upper part of the core compared to the middle and lower parts of the core. In order to reconstruct the past vegetation and climate changes of surrounding landmass, we calculated the paleoclimatic coefficient (Kp). The Kp is a ratio of total percentages of warm species (for example, dark conifer *Picea* sect. *Omorica* and *Picea* sect. *Eupicea* (spruce) and broadleaves — *Quercus* (oak), *Yuglans* (walnut) and *Ulmus* (elm)) and cold species (such as *Duschekia* (alder)). These species were used because their pollen percentages varied significantly in the investigated core. *Quercus* and *Ulmus* are major elements of broadleaved forest in the studied region at the present according to the map in the Primorsky vegetation region (Lavrenko, 1964). *Picea* forms dark coniferous vegetation and has a wide-spread occurrence. *Duschekia* characterizes the vegetation of the northern areas with cold climate conditions. Therefore, high Kp values are related to vegetation formed under a warm climate and vice versa.

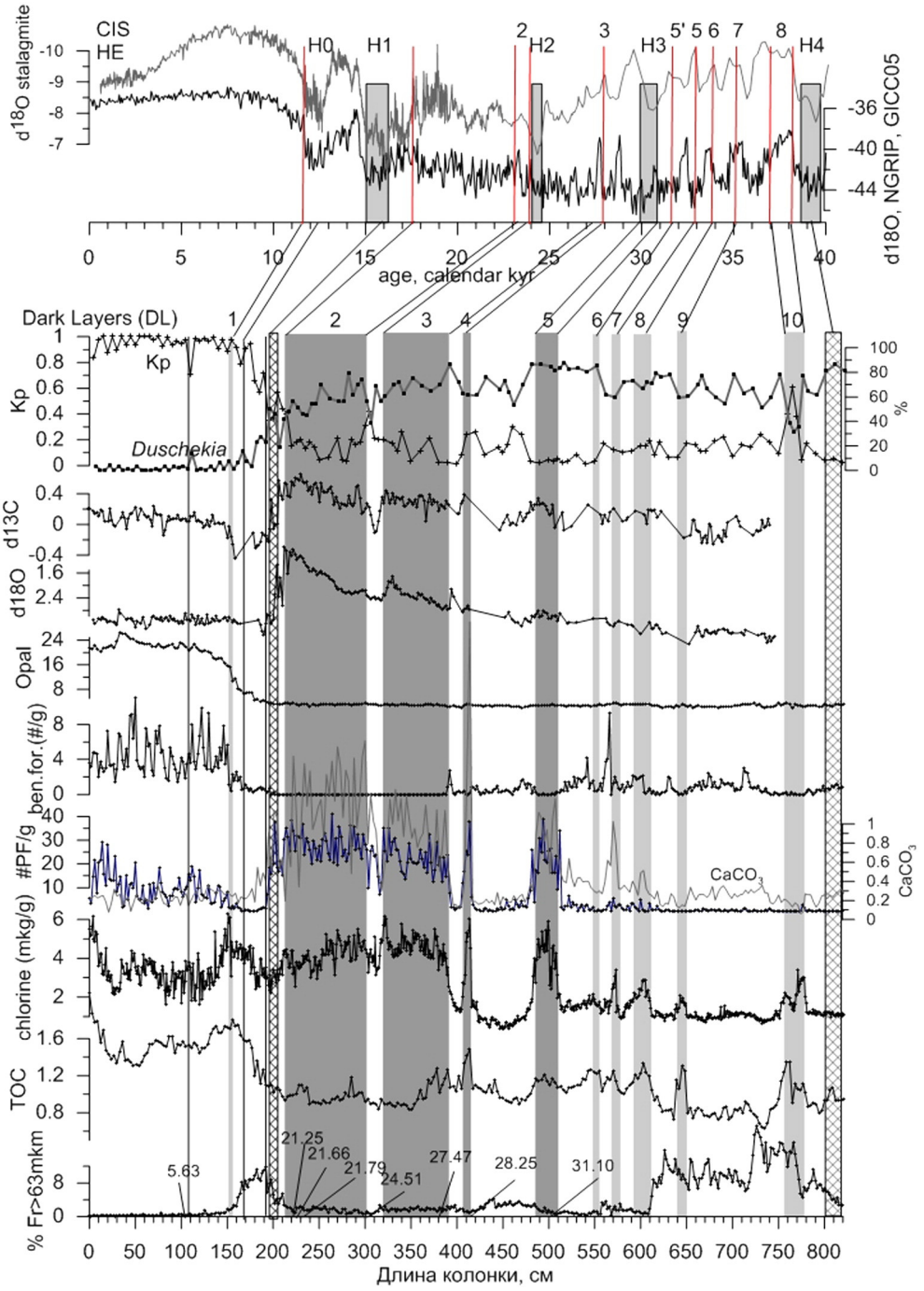

Fig. 2. Depth profiles of proxy records obtained from core LV 32–33 investigated in this study: IRD (weight % of coarse fraction (63 μm–2000 μm)), total organic carbon (wt.%) and chlorine content (μg/g sediment), number of the planktonic and benthic foraminifera (# shell/g sed.), opal and $CaCO_3$ content (wt.%), $\delta^{18}O$ and $\delta^{13}C$ of the planktonic foraminifera *N. pachyderma* sin. (‰ relative to PDB), climatic coefficient Kp and % of cold species of *Duschekia* in shrub-tree group. Also included are $\delta^{18}O$ records of Chinese cave stalagmite (Wang et al., 2008) and $\delta^{18}O$ of the Greenland ice core (NGRIP members, 2004) versus age (calendar ka) for comparison. AMS ^{14}C dates of core LV 32–33 (calendar ka) are shown at the bottom. Shaded bars mark the DLs 10–6, 1 and dark shaded bars—the thinly laminated DLs 5–2. Chinese interstadials (CIS) and cold Heinrich event (HE) are shown at the top.

Total carbon and inorganic carbon ($CaCO_3$) contents of sediments were measured at 1 cm intervals by a coulometric analyzer (AN-7529) (Gorbarenko et al., 1998). Total organic carbon (TOC) content was calculated from the difference between total carbon and inorganic carbon contents.

Opal content in sediments was analyzed following the method of Mortlock and Froelich (1989) described also in Gorbarenko et al. (2004). The chlorine content, the transformation product of chlorophyll-a in sediments, was measured with a Shimadzu UV–vis-NIR spectrophotometer (UV-3600) according to the modified method of Harris et al. (1996).

Ice rafted debris (IRD) content in the studied core was measured as weight percentage of the fraction 63 μm–2000 μm in the carbonate free dry sediments (Conolly and Ewing, 1970; Sakamoto et al., 2005). According to binocular testing control, material of this fraction is presented mostly by terrigenous particles, which were delivered to the core area by the sea ice drifting and its melting during summer seasons.

Table 1
AMS ^{14}C data on monospecies planktonic foraminifera *N. pachyderma* sin. for core LV 32–33. All measured ^{14}C age data were corrected by Japan (East) Sea surface water reservoir ages of 400 years (Yokoyama et al., 2007). All radiocarbon ages were converted into calibrated 2-sigma calendar age ranges using the calibration program CALIB REV 7.0.1 (Stuiver and Reimer, 1993) with the Marine 13 calibration curve (Reimer et al., 2013).

Accession #	Depth (cm)	Foram species	AMS ^{14}C age (yrs BP)	Error (±yr)	Cal. age (ka BP)
KIA 34207	105	*N. Pachyderma* sin.	5235	40	5.63
KIA 34208	202.5	*N. Pachyderma* sin.	16,850	100	19.90
KIA 34209	212.5	*N. Pachyderma* sin.	17,520	110	20.73
KIA 34210	226.5	*N. Pachyderma* sin.	18,250	120	21.66
KIA 34211	300.5	*N. Pachyderma* sin.	20,660	150	24.51
KIA 34212	380	*N. Pachyderma* sin.	23,590	170	27.47
KIA 34213	412	*N. Pachyderma* sin.	24,530	240	28.28
KIA 34214	500	*N. Pachyderma* sin.	27,440	330	31.10
OS-102816	222-1	*N. Pachyderma* sin.	18,000	80	21.33
OS-102817	222-2	*N. Pachyderma* sin.	17,850	70	21.17
OS-102671	232-2	*N. Pachyderma* sin.	18,350	65	21.79

Benthic and planktonic foraminiferal (BF and PF, respectively) abundance in sediments were counted under binocular and measured as number of shells per gram of natural dry sediment.

4. Results

4.1. Isotope-geochemical and lithological results

Fig. 2 shows depth profiles of important productivity proxies such as TOC, chlorine, opal contents and abundances of planktonic and benthic foraminifera in the sediment core LV 32–33. Also included in Fig. 2 are the IRD variability, values of $\delta^{18}O$ and $\delta^{13}C$ of planktonic foraminifera, and pollen results—paleoclimate coefficient Kp and percent of cold species *Duschekia* in arboreal group.

In addition to observed three thinly laminated DLs (212–391 cm, 407–417 cm, and 485–510 cm) and dark layers determined in the course of sediment description, we used productivity and lithological proxies in order to be more precise in defining the location of DL layers 1–10 in the studied core. The determination of DL layers is based on Tada et al. (1999)'s criteria with higher organic component content — TOC, chlorine and $CaCO_3$ except for MIS 2 (shaded bars, Fig. 2). It was suggested that the formation of DL layers under suboxic to euxinic surface sediment condition also leads to good preservation of PF, but barren BF; however BF content at the base of following light layers, formed under higher oxygen content, sharply increased with respect to dark/light layer transition (Oba et al., 1991; Tada et al., 1999). An interval of 151–156 cm had higher values of chlorine and TOC, followed by increased BF content which is likely to be correlated with earlier identified DL 1 in the Japan (East) Sea (Tada et al., 1999; Yokoyama et al., 2007) (Fig. 2). DLs 2–10 in core LV 32–33 consistently correlated with the above mentioned productivity and foraminiferal occurrence criteria (Fig. 2). Lithological description was identified at an interval of 212 cm–391 cm, as a single thinly laminated layer in core LV 32–33 with high $CaCO_3$, PF abundance and chlorine content, lightest values of $\delta^{18}O_{pf}$ and absence of BF in sediment (Fig. 2). However, they may be separated as DL 3 and DL 2 based on the deviation in chlorine, PF abundance, $\delta^{18}O_{pf}$ and $\delta^{13}C_{pf}$ records (Fig. 2) at intervals of 212–302 cm and 319–391 cm, respectively. This is consistent with earlier founded dark layers 2 and 3 in the Japan (East) Sea (Tada et al., 1999; Yokoyama et al., 2007). The thinly laminated DLs 2–5 (Fig. 2, dark shaded bars) demonstrate the abundance of PF and absence of BF followed by increased numbers of BF, suggesting their survival responses with respect to dark/light layer transitions. DLs 6–9 are characterized by a lesser increase of the productivity proxies and PF content. However, they demonstrated all features related to DLs (Fig. 2, light shaded bars). DL 10 is clearly characterized by peaks of productivity indices such as TOC and chlorine contents.

4.2. Pollen results

All pollen taxa in core LV 32–33 were classified into three groups, arboreal (trees and shrubs), herbaceous and spores, and their variability against depth is shown in Fig. 3. Fig. 3 also includes two families of spores (Polypodiaceae and Sphagnum), dominant arboreal species and climate coefficient Kp. On the basis of dominant and subdominant arboreal species, shares of different groups in total pollen assemblage and Kp values, we demarcated 8 pollen zones in the studied core which allow us to demonstrate the evolution of regional vegetation in the past (Fig. 3).

Zone 8 *Duschekia–Betula* sect. *Albae* (interval 780–820 cm). The amount of spore increases in the overall composition, whereas percentage of arboreal and shrubs decreases. Pollen of *Duschekia* dominates (over 80%) in pollen assemblages. The Kp is low (on average, 0.1). This zone shows growth of vegetation mainly alder, which is typical of cold conditions (Fig. 2).

Zone 7 *Betula* sect. *Albae–Duschekia* (interval 750–780 cm). Pollen of arboreal and shrubs dominates the overall composition (63–86%). The pollen percentage of *Betula* sect. *Albae* decreases to 26%, *Duschekia* decreases almost twice of *Albae*, and *Quercus* pollen is singly observed. The Kp index is strongly increased. This zone characterizes climate warming.

Zone 6 *Duschekia–Abies–Betula* sect. *Albae* (interval 550–750 cm). Pollen of arboreal and shrubs dominates in the overall composition, *Duschekia* in this group has a large percent. Several peaks of *Abies* pollen (about 14% each) are noted in this zone. The Kp index is characterized by low values.

Zone 5 *Duschekia* (interval 480–550 cm). This zone is characterized by a percentage increase of arboreal and shrub pollen. Pollen of *Duschekia* reaches its maximal value for the whole core (81–88%). The average value of Kp is very low (0.05). This zone points to growth of tundra vegetation and cold condition in the region.

Zone 4 *Duschekia–Betula* sect. *Albae–Picea* (interval 215–480 cm).

Subzone 4c *Duschekia–Picea* sect. *Eupiceae* (interval 405–480 cm). Groups of arboreal and shrubs in the overall pollen composition increase appreciably, and pollen of *Duschekia* dominates (to 73%). Insignificant peaks of *Picea* sect. *Eupiceae* pollen are noted at the interval of 460 cm–410 cm and Kp in these intervals increases to 0.3. Subzone indicates the growth of alder and spruce.

Subzone 4b *Duschekia–Betula* sect. *Albae–Picea* sect. *Omorica* (interval 245–405 cm). Content of *Duschekia* pollen on average is about 70% in the group of arboreal and shrubs. Content of *Betula* sect. *Albae* pollen increases to 5–17% in comparison with subzone 4c. Content of *Duschekia* shows a sharply decreasing pattern, and content of fir and spruce is increasing at 305 cm. The Kp index reaches 0.4.

Subzone 4a *Duschekia–Picea* sect. *Omorica* (interval 215–245 cm). Pollens of *Duschekia* and *Betula* sect. *Albae* decrease in group of arboreal and shrubs. There is a low content of pollen *Picea* sect. *Eupiceae* and *Picea* sect. *Omorica* which both decrease down to 5%. There is appearance of a small percent of pollen of broad-leaved taxa. The value of Kp is the same as in subzone 4b.

Zone 3 *Duschekia–Quercus* (interval 195–215 cm). At 205–220 cm, *Duschekia* pollen decreases sharply down to 19%, whereas the content of *Betula* sect. *Albae* and *Picea* sect. *Omorica* pollen increases (19% and 20%, respectively). The value of Kp sharply increases. On the interval of 195–205 cm, the content of *Duschekia* pollen increases, while the contents of *Betula* sect. *Albae* and *Picea* sect. *Omorica* decrease. This zone indicates growth of alder, birch and spruce vegetation.

Subzone 2b *Quercus–Duschekia* (interval 165–195 cm). *Quercus* pollen sharply increases while *Duschekia* strongly decreases. The value of Kp sharply increases. This subzone indicates significant warming.

Subzone 2a *Quercus–Picea* sect. *Eupiceae* (interval 60–165 cm). *Quercus* dominates in the group of arboreal. In the interval of 110–150 cm, its content reaches maximal value up to 47% of the whole core. The presence of pollens *Juglans*, *Ulmus*, and *Tilia* is noted. Pollen of

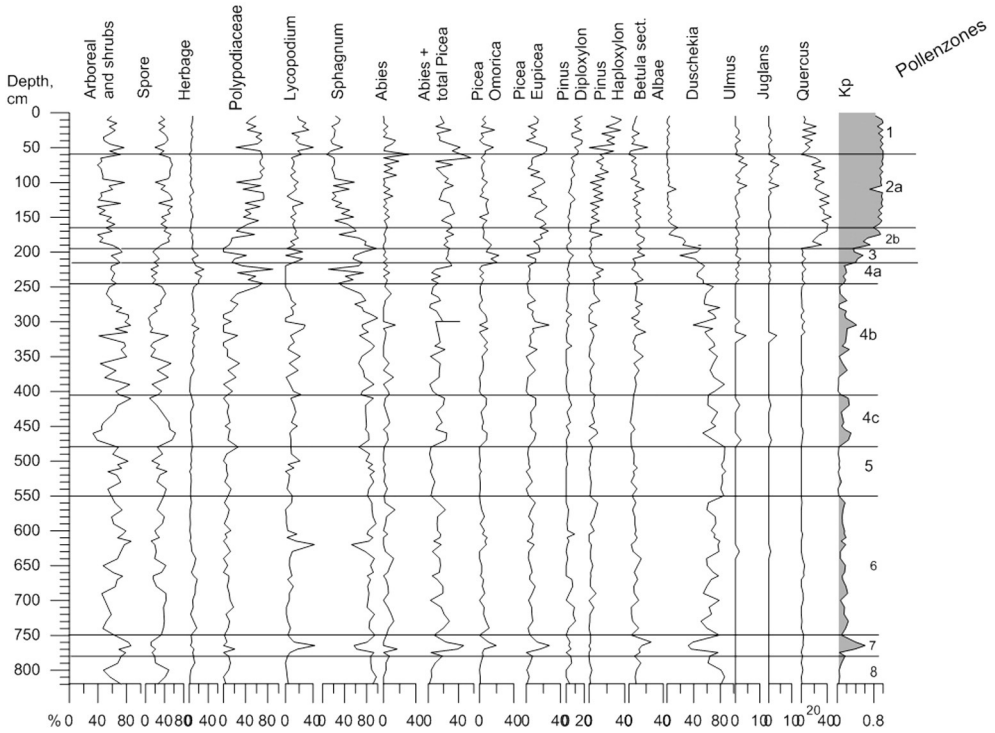

Fig. 3. Percentages of total pollen composition (arboreal plus shrubs), spore and herbs groups (%), 2 families of spores, percentages of pollen species of arboreal group and the paleoclimate coefficient Kp in core LV32–33 sediments against core depth. Also shown are major 8 pollen zones and sub-zones.

conifers (*Pice* sect. *Eupicea*, *Pinus* s/g *Haploxylon*, *Picea* sect. *Omorica*, *Pinus* s/g *Diploxylon*) is contained in a considerable amount. The value of Kp is high (0.95). This zone indicates the growth of mixed forest and warm climate conditions.

Zone 1 *Pinus* s/g *Haploxylon–Quercus* (interval 0–60 cm). This zone is characterized by high content of arboreal and shrub pollen and *Pinus* s/g *Haploxylon*. However, content of *Quercus* decreases, and *Juglans* and *Ulmus* are rare. The value of Kp does not change. Zone 1 indicates the growth of taiga and broad-leaved forest and cooler climatic conditions.

5. Age model

Age model of the core LV 32–33 was constrained by using AMS ^{14}C dating (Table 1). A correlation of well known DLs with its boundary ages of several dated cores in the Japan (East) Sea was used (Tada et al., 1999; Itaki et al., 2004; Yokoyama et al., 2007; Table 2) and a correlation of the DL 5 and DL 10 with prominent vegetation/climate DO cycles was determined by pollen analysis of the same core sediment (Fig. 2).

As was mentioned earlier, DL 1 with age of 11.4 ka BP (Tada et al., 1999; Yokoyama et al., 2007) was estimated according to its maxima in productivity proxies in the interval of 151–156 cm (Fig. 2). In addition to Tada et al.'s (1999) hypothesis of the dark layer formation with high organic content during DO interstadials, we hypothesize that during deglaciation and after normalization of the Japan (East) Sea, surface water salinity (after 18–17 ka BP), formation of light layer (LL) in the interval of 196–206 cm with minima of productivity proxies (TOC and chlorine) was related to a more severe climate condition of DO stadial equivalent to HE 1 (Fig. 2). Age of HE 1 might be correlated with Greenland ice core δ^{18}O record (NGRIP members, 2004; Wolff et al., 2010) and with the best dated Chinese stalagmite δ^{18}O curves (Wang et al., 2001; Wang et al., 2008) (Table 3).

Decreased PF abundance above 212 cm indicates partial dissolution of the foraminiferal tests. In addition, some older foraminifera from sediments below 212 cm may have disturbed the upper sediment as a result of bioturbation. These effects may bias the initial ages of the sediments above 212 cm. Four AMS ^{14}C dates from the upper part of DL 2 with high abundance of foraminifera tests, measured on undissolved planktonic foraminifera in two different laboratories, show a sequence of reliable results (Table 1). This is why we reject the AMS ^{14}C data measured at depths of 202 and 212 cm with ages of 19.9 and 20.73 ka BP, respectively: in addition, there are possibilities changing radiocarbon including reservoir ages due to environmental changes such as hydrological changes (Matsumoto and Yokoyama, 2013). We accept the average age of doubled dated interval of 222 cm to be 21.25 ka BP as a key time point of upper part of DL 2 (Table 3). It is notable that age of DL 2 top at depth of 212 cm (18.6 ka BP), calculated by interpolation between tie points of 15.7 ka BP and 21.25 ka BP may be slightly younger than the original due to small sedimentation rate between these tie points compared with one of lower interval.

Table 2
Ages (calendar ka) of dark/thinly-laminated layers (DL) according to Yokoyama et al. (2007), Itaki et al. (2004) and Tada et al. (1999) with the studied core numbers.

DL number	Yokoyama et al. (2007) D-GC-6, MD01-2407	Itaki et al. (2004) GH-96-1217, KT94-15-PC9	Tada et al. (1999) Site 797, KH79-3
2 top	17.40	15.60	17.67
2 bottom	23.10		22.15
3 top	23.8		
3 bottom	27.3		25.25
4 bottom	28.6	26.50	26.66
AT ash			29.24
5 bottom	31.60	31.00	30.32
6 bottom			31.08
7	?34.20[a]		32.07
8 top		32.5	
8 bottom	?37.4[a]		34.63
9 bottom			36.72
10 middle			
10 bottom			38.14

In this case the ages are closed to reality.
[a] Seems to be that Yokoyama et al. (2007) mean DLs 7 and 8 as dark layers, correlated with DOIs 7 and 8.

Table 3
AMS ^{14}C data, position of marker horizons with its accepted age (cal. ka) and age model key time points in core LV 32–33. Age model of the core LV 32–33 was constrained by using accepted AMS ^{14}C dating, correlation of well known DLs with its boundary ages of several dated cores in the Japan (East) Sea (Tada et al., 1999; Itaki et al., 2004; Yokoyama et al., 2007) and correlation of the DLs with prominent vegetation/climate DO cycles determined by pollen analysis.

Core depth (cm)	Marker horizons	AMS ^{14}C age (ka)	Accepted ages of marker horizons (cal. ka)	Age model key time points (cal. ka)
105		5.63		5.63
151	DL 1 top			
153.5	DL 1 middle		11.4	11.4
156	DL 1 bottom			
166	YD cooling			
195	HE 1 top			
199	HE 1 middle		15.7	15.7
203	HE 1 bottom			
202.5		19.9?		
212	DL 2 top			
212.5		20.73?		
222		21.25		21.25
226.5		21.66		
232		21.79		
300.5		24.51?		
302	DL 2 bottom/DOI 2 top		23.1	23.1
319	DL 3 top/DOI 2 bottom		23.8	23.8
380		27.47		
391	DL 3 bottom		27.3	27.3
407	DL 4 top			
411	DL 4 middle/DOI 3		27.8	27.8
412		28.25		
485	DL 5 top/HE3 top		29.9	29.9
500		31.10		
517	DL 5 bottom/HE 3 bottom		30.9	30.9
550	DL 6/DOI 5′		31.6	31.6
572	DL 7/DOI 5		32.9	32.9
600	DL 8/DOI 6		33.8	33.8
644	DL 9/DOI 7		35.1	35.1
755	DL 10 top/DOI 8 top		36.9	
766.5	DL 10 middle/DOI 8 middle			37.55
778	DL 10 bottom/DOI 8 bottom		38.2	
801	DOS 9 top			
801.5	DOS 9 middle		39.3	39.3
818	DOS 9 bottom			

We accept ages of DL 2 bottom, DL 3 boundaries according to the well dated core D-GC-6 (Yokoyama et al., 2007) (Table 2). DL 4 correlated with GIS/CIS 3, consistently with Tada et al.'s (1999) hypothesis and pollen results (Fig. 2), indicating its time formation (27.8 ka BP) which is rather close to the age estimations of Tada et al. (1999) and Yokoyama et al. (2007) (26.6 ka BP and 28.6 ka BP, respectively). Some older ages of the AMS ^{14}C data measured in the studied core as compared with those of Yokoyama et al. (2007) are probably connected with the increase of reservoir age in subsurface water of the Japan (East) Sea during low sea level standing and increased surface water stratification.

In order to correlate some DLs with related regional climate conditions, we used also pollen results of studied core sediments (paleoclimate coefficient Kp and percentages of cold species *Duschekia* in arboreal group) to reconstruct a more prominent regional vegetation/climate oscillations during some DLs (Fig. 2). Available pollen data clearly indicates significant climate cooling during DL 5 formation and strong warming during DL 10 (Fig. 2). The vegetation/climate trend in the studied core allows us to correlate DL 5 with cold HE 3. AMS ^{14}C age measured in the middle of DL 5 (31.10 ka BP) and available radiocarbon dating of DL 5 in other cores (Tada et al., 1999; Yokoyama et al., 2007) had a rather close time of such prominent climate stadial. Significant vegetation/climate amelioration during DL 10 may be correlated with pronounced long-lasting climate warming of GIS/CIS 8 which is close to the time suggested by Tada et al. (1999) (38.14 ka). DLs 9–7 are probably correlated with GIS/CIS 7–5 respectively. DL 6 is likely related to the following them less pronounced interstadial, visible in records of $\delta^{18}O$ in Greenland ice core and Chinese cave stalagmite with age of 31.5 ka BP, which may be referred as GIS/CIS 5′. We correlated a light interval of 819–801 cm formed during the regional climate cooling (and preceded GIS/CIS 8) with cold stadial GS/CS 11 equivalent to HE 4 (Fig. 2).

Fig. 4 shows a relation of core depth–age of key points determined by above mentioned ages of DLs 1–10 and accepted and rejected AMS ^{14}C ages for this core. Ages of sediments deposited between key time points were calculated by interpolation.

6. Discussion

6.1. Dark–light layer formation — the Japan (East) Sea environment–regional climate changes

Since the surface and bottom water condition and therefore DL formation in the Japan (East) Sea is strongly determined by water exchange with the west Pacific and regional precipitation influencing the surface environments and nutrients input to the sea, we compared the obtained results for core LV 32–33 in the established age model with excellent dated record of East Asian monsoon intensity (Wang et al., 2008) and sea level changes in Arz et al. (2007) (Fig. 5). Several early important works such as Heusser and Morley (1985), Kawahata et al. (2011) and Igarashi et al. (2011) were devoted to investigating the connections of terrestrial-ocean environmental changes in the northwestern Pacific. However pollen investigation of core LV 32–33 provides the first high-resolution vegetation records from the northern Japan (East) Sea sediments with established DLs. These high-resolution vegetation records on the basis of pollen analyses of well dated core were also used to clarify correlation of DL formation with regional millennial scale climate and sea level changes (Fig. 5). We used immediate type of vegetation responses to regional climate changes and accepted the time of vegetation regional response equal to around 150 years (Chapin and Starfield, 1997). That is why the records of pollen proxies in Fig. 5 were shifted on 0.15 ka BP to the right in the time scale.

Vegetation of surrounded land in sediments of the studied core base (interval 801–819 cm) indicated cold climate conditions of the Japan (East) Sea coeval to HE 4. Decreased East Asian summer precipitation (Wang et al., 2001) and weak nutrient input into the sea through the Tsushima Strait lead to a low productivity during this period. High IRD values were evident that sea ice covered this northern region during the winter seasons and a lot of IRD thus accumulated at the bottom during summer sea ice melting. Low PF abundance and $CaCO_3$ content, is likely related to poor carbonate preservation suggesting suboxic bottom water condition and moderate deep ventilation that allow surviving of benthic foraminifera (Fig. 5).

As mentioned above, sediments of DL 10 were formed during abrupt, long-lasted climate warm periods of GIS/CIS 8 at ~37–38 ka BP according to pollen records and peaks of Kp coefficient (Figs. 2 and 5). The formation of DL 10 with high TOC and chlorine contents is consistent with the hypothesis of Tada et al. (1999), who attributed the dark layer formation to increased East Asian summer monsoon with precipitation transferring and related input of nutrient-rich ECSCW water into the Japan (East) Sea (Fig. 5). Several cores from the south eastern part of the Japan (East) Sea also demonstrate high productivity and oxygen deficit in sediments of DL 10 according to sediment fabric classification (Watanabe et al., 2007). Some decrease in $CaCO_3$ content and in BF occurrence in sediments of DL 10 (Fig. 5) consistent with Watanabe et al. (2007) indicates that decrease in dissolved oxygen in the sediments may be related with oxygen consumption under increased organic matter input into the bottom. However, the bottom water ventilation, most likely, did not change significantly.

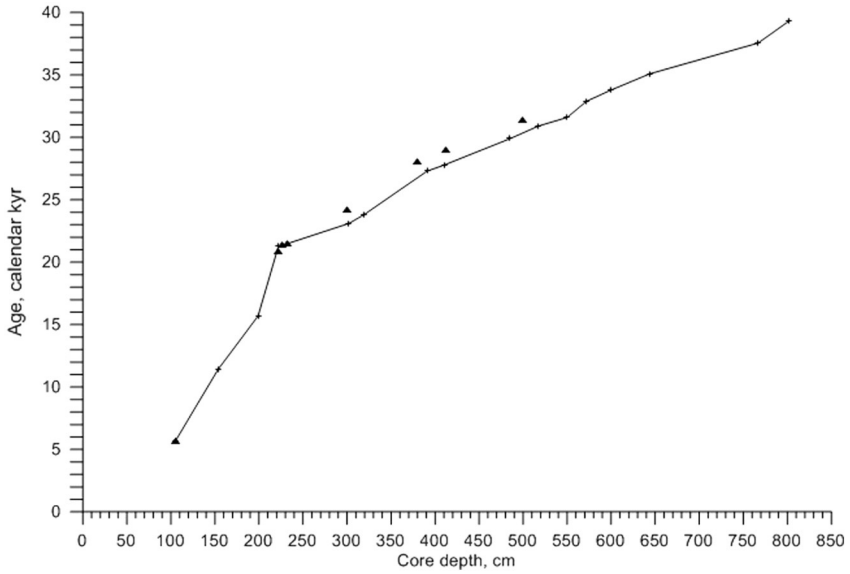

Fig. 4. Age–depth relationship for core LV 32–33 age model based on the key time points (Table 3, crosses). AMS ^{14}C data are shown by triangles.

Warming of long-lasted GIS/CIS 8, intensified summer seasons melting the sea ice burdened with terrigenous sediments, caused violent accumulation of IRD on the bottom for 38–34 ka BP. Percentages of coarse fraction of >63 μm in sediments during this time interval increased up to 12–15 weight percentage compared with nearly 2% of late MIS 3 and MIS 2 and with 0.2% for Late Holocene. The result initiated by climate warming, sea ice melting and intensification of sedimentary processes, increased the sedimentation rate up to 40–50 cm/kyr. It is notable that IRD records estimated in core GH95-1208, located in the south of the studied core LV32-33 (Fig. 1), demonstrate also strong IRD peak since DOI 8 (37.5 ka BP) (Ikehara and Itaki, 2007), indicating significant changes in the sea ice formation, its drifting and melting during this time period.

The higher TOC and chlorine contents during DLs 9, 8, 7 and 6 formation suggest the increased sea-surface productivity consistent with sequence of intensifications of summer East Asian monsoon recorded in the China stalagmites (Figs. 2 and 5). Very low PF and BF occurrence in sediments during DL 9 and small increase for layers of DL 8 and 7 indicate that ventilation of the bottom water was moderate and did not change significantly, consisting with rather high sea level standing. Available pollen results do not show significant vegetation/climate changes during this time span. DL 5 well defined by strongly increased TOC and chlorine contents is characterized by thinly laminated accumulation, absence of benthic foraminifera and abundance of planktonic foraminifera. The dominance of cold and dry preferred species in pollen records and very low Kp coefficient, show the prevalence of cold climate during that interval, most likely, correlating to the North hemisphere prominent stadial Heinrich event 3 (Figs. 2 and 5). Lowering of global sea level after 31 ka BP (Fig. 5; Arz et al., 2007) caused the reduction of the Japan (East) Sea water exchange with the saline Pacific water, intensified surface water freshening and consequently weakened deep water ventilation that in turn lead to deficit of dissolved oxygen, euxinic condition in sediments and low organic matter decomposition. Planktonic foraminifera content being low in sediments of core base strongly increased in DL 5, indicating well preservation of carbonate tests under euxinic surface sediment conditions, consistent with barren benthic foraminifera and formation of thinly laminated sediment.

Pollen record shows two warm climate events after the deposition of DL 5 at intervals nearly of 470 cm (29 ka BP) and nearly of 415 cm (28 ka BP) that seems to be correlated with GIS/CIS interstadials 4 and 3, respectively. However, only upper interval, identified as DL 4, is characterized by increased TOC, chlorine, $CaCO_3$, PF contents and thinly laminated sediment consistent with lower sea level standing (Figs. 5 and 6).

The formation time of DLs 2 and 3 (Table 3) coincides with the interval of sea level dropping to the lowest stand according to Arz et al. (2007) (Fig. 5). During those intervals, maximal surface water freshening indicated by the lightest $\delta^{18}O_{pf}$ resulted in maximal surface water stratification and further bottom water stagnation, due to strong decrease of saline Pacific water inflowing into the sea (Oba et al., 1991; Gorbarenko and Southon, 2000). Very high abundance of PF and maximal $CaCO_3$ values together with complete barrenness of BF in these DLs indicate extreme euxinic condition in the surface sediments on the sea floor. However, in spite of euxinic condition of DLs 3 and 2, TOC values were low, while chlorine content shows higher values. High values of IRD and chlorine contents in sediments of DLs 2 and 3 indicate seasonal sea ice covering in the studied northern area and summer ice free conditions that induced increase in phytoplankton production within surface water and IRD accumulation on the bottom. The sediments between the DL 2 bottom and DL 3 top, based on deviation of productivity proxies (chlorine and $CaCO_3$ contents), PF abundance and $\delta^{18}O_{pf}$ and $\delta^{13}C_{pf}$ seemed to be accumulated during some regional abrupt warming of GIS/CIS 2. This is strongly corroborated by pollen results (Figs. 2 and 5), showing some amelioration of vegetation simultaneously with DO/C interstadial 2.

Coeval to the upper boundary of DL 2, sharp increase in $\delta^{18}O_{pf}$ at 18.6 ka BP indicates strong increase of surface water salinity consistently with enhanced Pacific water inflow into the Japan (East) Sea due to global abrupt sea level rise (Fig. 5). With small delay, after $\delta^{18}O_{pf}$ increase, abrupt decrease in the $\delta^{13}C_{pf}$ is observed in the studied core (Figs. 2 and 5) and other Japan (East) Sea cores (Kim et al., 2000). Probably, the warm Tsushima Current together with the saline water of the cold Oyashio Current, with low $\delta^{13}C$ of $\sum CO_2$ (Kroopnick, 1985), flows into the Sea through the Tsugaru Strait during sea level rise (Oba et al., 1991; Gorbarenko and Southon, 2000). Increased Pacific water inflowing into the Japan (East) Sea after 18.6 ka BP transports heat to the sea which induced regional vegetation and climate amelioration, interrupted by cold event equivalent to HE 1 during 16.2–15.2 ka BP. This is consistent with available pollen results (Figs. 2 and 5).

Decreased PF abundance, paralleled with reduced $CaCO_3$ content, after the pulse of the Pacific water input at about 18.5 ka BP, most likely, indicates the start of ventilation. However, following slight increase of PF abundance, $CaCO_3$ content and complete absence of benthic foraminifera at interval correlated with cold HE 1, the evidence has strong deficits of dissolved oxygen at the bottom environments (Fig. 5). The following Bolling/Allerod (BA) warming, indicated by pollen data, has a very low PF abundance and decreased in $CaCO_3$ content, which suggests slightly improved bottom water ventilation resulting in carbonate

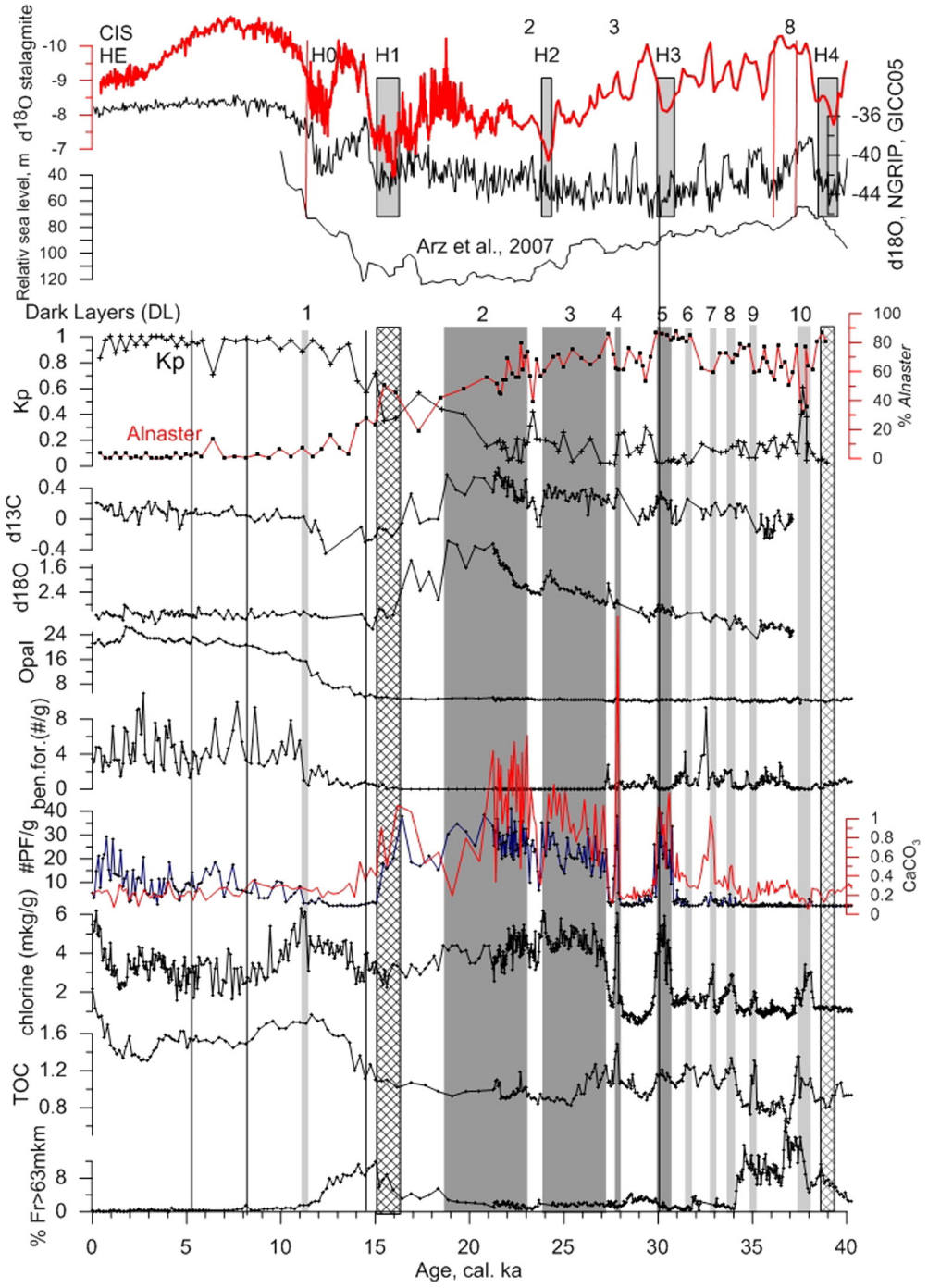

Fig. 5. Time correlation of the Chinese Interstadials of the East Asian monsoon variability (Wang et al., 2008), DO interstadials in $\delta^{18}O$ of the Greenland ice core ((NorthGRIP members, 2004) and sea level changes (Arz et al., 2007) with records of core LV 32–33 from the northern Japan (East) Sea core LV 32–33; IRD (wt.% of coarse fraction (63 μm–2000 μm)), total organic carbon (wt.%) and chlorine content (μg/g sediment), number of the planktonic and benthic foraminifera (# shell/g sed.), opal and $CaCO_3$ content (wt.%), $\delta^{18}O$ and $\delta^{13}C$ of the planktonic foraminifera *N. pachyderma* sin. (‰ relative to PDB), climatic coefficient Kp and % of cold species of *Duschekia* in shrub-tree group. Hatched rectangular bars denote the H1 and H4 cold events. Other rectangular bars are similar to Fig. 2.

dissolution consistent with heavy $\delta^{18}O_{pf}$ values and increase of BF occurrence in sediments (Fig. 5). Regional environment amelioration in the northern Japan (East) Sea, coeval to BA warming, significantly intensified over the summer sea ice melting, causing large amounts of IRD accumulation. Following the BA warming, cold Younger Dryas event (HE 0), was marked by vegetation shift to cold climate-preferred pollen species and significant decrease in $\delta^{13}C$ of planktonic foraminifera.

According to pollen results and strong decrease in sea ice influence indicated by IRD records, regional climate warming in the northern Japan (East) Sea was established at the beginning of Holocene (Figs. 2 and 5). However, BF production during DL 1 formation was hampered, most likely due to intensive oxygen consumption which resulted from increased organic decomposition in the surface sediments (Fig. 5). Complete renewal of deep water ventilation in the Japan (East) Sea related with modern type surface water Currents was established after DL 1 formation, indicated by increased $\delta^{13}C_{pf}$ values in the studied core and southern cores (Kim et al., 2000). In turn, strong deep water ventilation brought nutrients from deep water reservoirs to euphotic layer and caused an increased productivity in the surface water (Fig. 5). On the other hand, a strong increase of East Asian summer monsoon at the

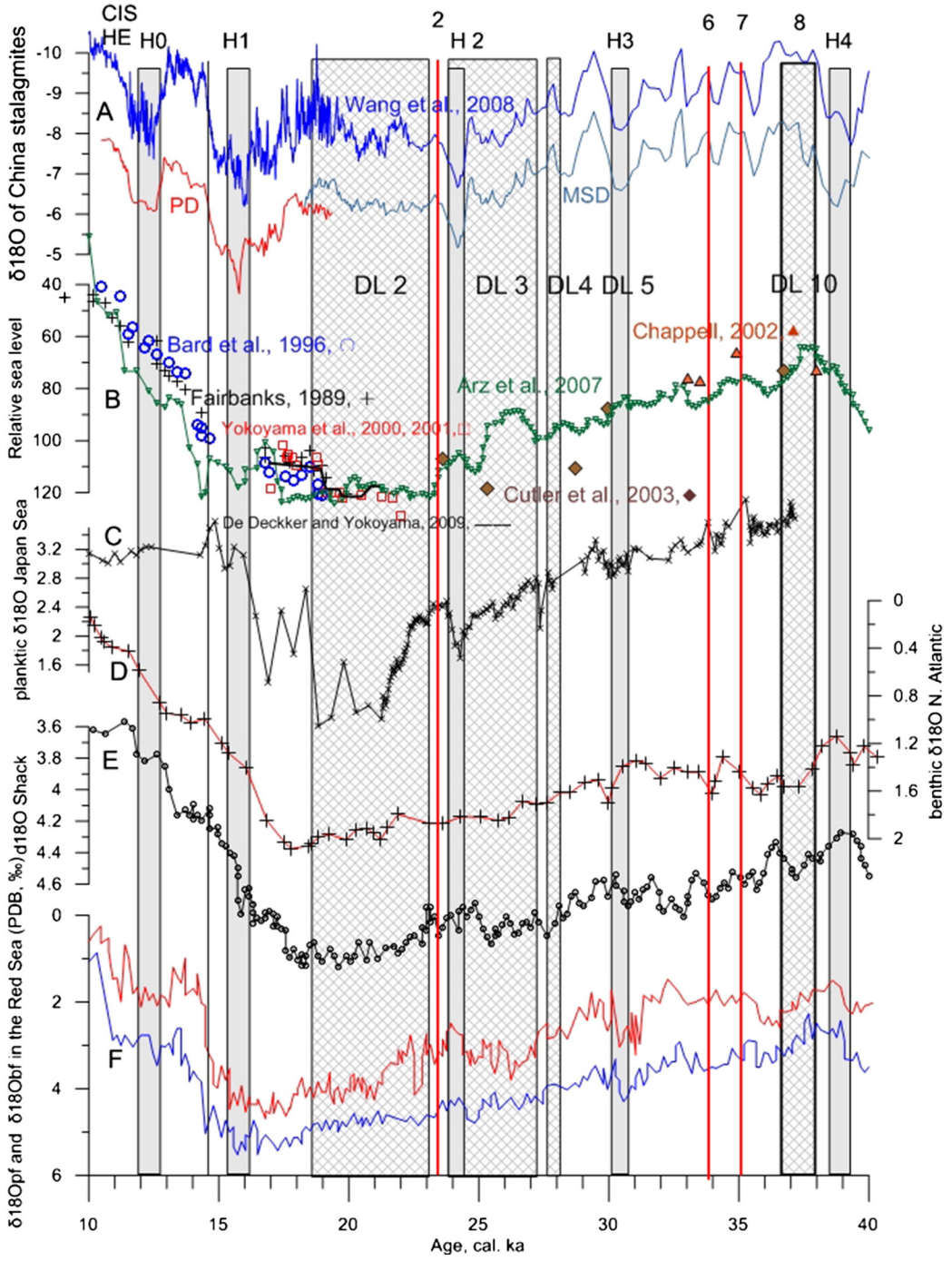

Fig. 6. In time comparison of the Japan (East) Sea $\delta^{18}O$ planktonic foraminifers record with other related sea level change records and with millennial cycles of East Asian monsoon over 10–40 ka BP. A—$\delta^{18}O$ records of the Chinese stalagmites (Wang et al., 2001; Wang et al., 2008); B—relative sea level estimates: reconstruction from the northern Red Sea based on the benthic $\delta^{18}O$ record considering alkenone corrections for the sea surface temperature (Arz et al., 2007), sea-level estimates of U–Th and ^{14}C dated corals from Barbados and Papua New Guinea (cross, Fairbanks, 1989; rhomb, Cutler et al., 2003), from the Thaiti (circle, Bard et al., 1996), from the Huon Peninsula (triangle, Chappell, 2002), and of ^{14}C dated carbonate remnants from Bonaparte Gulf, Australia (square, Yokoyama et al. (2000, 2001), black line—De Deckker and Yokoyama (2009); C—J/ES $\delta^{18}O$ planktonic foraminifers measured in this study; D—benthic $\delta^{18}O$ record of North Atlantic core of NA 87–22 compiled by Waelbroeck et al. (2002); E—benthic $\delta^{18}O$ record from core MD 95–2042 located at the Iberian margin (Shackleton et al., 2000) on the SFCP 2004 time scale (Shackleton et al., 2004); F—planktonic and benthic $\delta^{18}O$ records from the Red Sea core GeoB (Arz et al., 2007). Gray bars denote the HE, hatched bars–DL 2, 3, 4 and 10. (For interpretation of the references to color in this figure legend, the reader is referred to the web version of this article.)

beginning of Holocene around 11.4 ka BP (Wang et al., 2001; Fig. 5) supplied additional nutrients from Huanghe and Changjiang rivers running off into the sea, also promoting increase in surface water productivity. Notably that strong increase in opal accumulation since DL 1 formation that influenced productivity, had occurred together with sharp drops in IRD accumulation and weaker sea ice cover, similarly observed as in the Okhotsk Sea (Gorbarenko et al., 2014). Perhaps, siliceous phytoplankton productivity (mostly by diatom production) in both basins was related with intensity of spring sea ice melting and surface water stratification.

6.2. $\delta^{18}O$ of planktonic foraminifera relationship with global sea level changes

$\delta^{18}O$ of planktonic foraminifera recorded from the Japan (East) Sea ($\delta^{18}O_{pf}$) shows a strong negative excursion during the last glacial

maximum, interpreted as a strong decrease in surface water salinity due to weaker inflowing saline Pacific water resulting from the descent of sea level (Gorbarenko 1983, 1993; Oba et al., 1991, 1995). The unique sensitivity of the Japan (East) Sea environment to global sea-level changes is a consequence of its restricted connection with the North Pacific Ocean through the narrow and shallow Tsushima and Tsugaru Straits (sill depth of 137 m). This situation is similar to responses of the Red Sea, which is located in an arid climate zone, contrary to the Japan (East) Sea located which is in a humid temperate climate zone. Therefore, $\delta^{18}O_{pf}$ in the former basin (the Red Sea) increased with lower global sea level due to high evaporation and increase in salinity (Siddall et al., 2003), and decreased in the latter basin (the Japan (East) Sea) due to excess of precipitation over evaporation, freshening of sea-surface water and therefore, its reduced salinity resulted from large amounts of riverine discharge from surrounding hinterlands. Therefore, high resolution $\delta^{18}O$ records of planktonic foraminifera of the studied sediment core may provide useful evidence for global sea level changes during the late Quaternary glacial–interglacial cycles.

According to the paleotemperature scale (Epstein et al., 1953), $\delta^{18}O$ values of foraminiferal calcite shell are determined by $\delta^{18}O$ of ambient water and water temperature during shell formation. We assume that planktonic species *Neogloboquadrina pachyderma* (sin.) formed their shells in the studied area, as well as in the Okhotsk Sea, above or slightly below the thermocline (Bauch et al., 2002) with modern water summer salinity of nearly 34.0‰ (Gydrometeorologiya and gydrochimija morej, 2003). Taking into account the relationship of water salinity–oxygen isotope found in the Okhotsk Sea (Keigwin, 1998), modern $\delta^{18}O$ of ambient water is nearly −0.3‰ relative to SMOW. Given this value of $\delta^{18}O_w$, the $\delta^{18}O_{pf}$ value measured in late Holocene, equaling to 3.2‰ (Fig. 2) corresponds to temperature of ambient water of nearly 3–4 °C according to revised paleotemperature results for species of *N. pachyderma* of Bemis et al. (1998). This calculated temperature is close to modern data for the studied area and depth (Gydrometeorologiya and gydrochimija morej, 2003). Thus, decrease in 1–2 °C of water temperature at depth habitation of studied planktonic foraminifera during glaciation corresponds, probably, to increase in the glacial $\delta^{18}O_{pf}$ up to 0.35‰. Global increase in $\delta^{18}O$ of water during glaciation went up to 1.05‰ (Duplessy et al., 2002) and temperature-driven changes in $\delta^{18}O_{pf}$ rose to +0.35‰, summing up to 1.4‰, but they have to decrease the negative maximal shift in $\delta^{18}O_{pf}$ during LGM, caused by sea level changes. So, observed changes in $\delta^{18}O_{pf}$ in the studied core from +3.2‰, during Holocene and in the period of 30–40 ka BP, descended to 1.07‰ during the LGM. Indeed, the sensitive responses of the Japan (East) Sea environment reflect the global sea level changes with maximal amplitude of up to 3.5‰ during this time span at sea level standing below 80 m of the modern one.

The trend of $\delta^{18}O_{pf}$ changes in core LV 32–33 from 32 to 15 ka BP resembles that of $\delta^{18}O$ records of planktonic and benthic foraminifera from the Red Sea (Arz et al., 2007), benthic $\delta^{18}O$ ($\delta^{18}O_{bf}$) curve from core MD 95-2042 recovered off southern Portugal (Shackleton et al., 2000, 2004), and $\delta^{18}O_{bf}$ recorded relative to the modern $\delta^{18}O_{bf}$ value (3.32% PDB) of the North Atlantic core NA 87-22, compiled by Waelbroeck et al. (2002) (Fig. 6). The trend of studied core $\delta^{18}O_{pf}$ also resembles the sea-level reconstruction from the northern Red Sea based on the benthic $\delta^{18}O$ record, considering the alkenone corrections for the sea surface temperature (Arz et al., 2007), sea level estimates from U–Th, ^{14}C dated corals from the Barbados, Papua New Guinea, Thaiti and Huon Peninsula (Fairbanks, 1989; Bard et al., 1996; Chappell, 2002 Cutler et al., 2003) and ^{14}C dated carbonate remnants from the Bonaparte Gulf, Australia (Yokoyama et al., 2000, 2001; De Deckker and Yokoyama, 2009) (Fig. 6). Since environmental variability of the Japan (East) Sea is tightly connected with global orbital and abrupt climate changes, again, we tested the correlation between the $\delta^{18}O_{pf}$ record with the best dated East Asian monsoon cycles measured in the China caves (Wang et al., 2001; Wang et al., 2008) (Fig. 6). We observed a slight decrease in the $\delta^{18}O_{pf}$ at 31–30 ka BP, which seems to be correlated with decreased sea level in the Red Sea and the North Atlantic. According to the pollen data this event might have initiated the DL 5 formation during cold HE3 (Fig. 6). After MIS 3 the first significant descent of global sea level started at 30–29 ka BP in accordance to changes of the Japan (East) Sea $\delta^{18}O_{pf}$ and other above mentioned results. In the period of 29–24.5 ka BP, the continuous decrease of sea level was observed in all of the records and was, possibly, interrupted by abrupt/slight drops nearly at 27.5 ka BP. Then $\delta^{18}O_{pf}$ record indicates clearly an abrupt decrease of sea level coeval to cold event HE 2, followed by significant increase in $\delta^{18}O_{pf}$ values indicative of fast sea-level rise coeval to DO/Chinese Interstadial 2. At the first half of DL 2 (24–22 ka BP) according to the $\delta^{18}O_{pf}$ changes, sea level went down considerably, which was consistent with most evidences and was nearly constant at minimum standing during 21 to 19 ka BP (LGM). Sharp increase in J/E $\delta^{18}O_{pf}$ values since 18.6 ka BP is consistent with available dated coral results from different regions (Fairbanks, 1989; Bard et al., 1996; Cutler et al., 2003). All of those data indicate that the LGM low stand was abruptly terminated by a rapid sea-level rise of 10 to 15 m at 19.0 ka BP. Clark et al. (2004) provide evidence for melt water pulse recorded at 19 ka BP in the North Atlantic that reduced the strength of North Atlantic Deep Water formation and forced attendant cooling of the North Atlantic at that time. Strong increase of $\delta^{18}O_{pf}$ was probably driven by further sea-level rise and occurred at 15.5–14.7 ka BP, close to the beginning of MWP-1A. The MWP-1A from the Sunda Shelf suggests a calendar age of about 14.6–14.3 ka BP (Hanebuth et al., 2000), which is earlier than that of U–Th dates from Barbados corals (Bard et al., 1990).

7. Conclusion

We investigated high resolution lithological, isotope-geochemical, micropaleontological and productivity sedimentary parameters of core LV 32–33 recovered from the northern Japan (East) Sea that allow us to distinguish 10 dark layers with high organic matter content over the last 40 ka BP. Results of pollen spectrum of the studied sediment core guide us to reconstruct the high-resolution vegetation changes of the surrounding land associated with glacial–interglacial and abrupt pronounced regional climate changes.

Age model of the core LV 32–33 was constrained by using accepted AMS ^{14}C dating (Table 1), correlation of well known DLs with its boundary ages of several dated cores in the Japan (East) Sea (Tada et al., 1999; Itaki et al., 2004; Yokoyama et al., 2007; Table 2) and correlation of the DLs with prominent vegetation/climate DO cycles determined by pollen analysis (Fig. 2). For instance, DL 10 was formed during the long-lasting GIS/CIS interstadial 8 at 38–37 ka BP and affected by the Huanghe and Changjiang rivers runoff with an accompanied influx of nutrient-rich ECSCW water into the Japan (East) Sea. This climate warming also caused regional sea ice melting in summer seasons, resulting in large IRD accumulation in the Japan (East) Sea. DL 5 formed at around 31–30 ka BP during cold HE 3 according to available pollen results, was most likely initiated by the global sea level descent (Arz et al., 2007) and reduction of seawater exchange with the saline North Pacific water and by weakening of deep water ventilation.

Decrease in the Tsushima Warm Current water inflowing was due to strong sea level descent during MIS 2 which led to freshening of the surface water and caused significantly decreased deep water ventilation. Under this euxinic bottom condition, DLs 2, 3 and 4 were formed with thinly laminated sediment.

Distinct rise in $\delta^{18}O_{pf}$ since 18.6 ka BP indicates abrupt increase in saline Pacific water inflowing and strengthening of deep water ventilation, due to sea level rise after LGM. Input of warmer Pacific water into the Japan (East) Sea brought heat and moisture to its northern part and induced vegetation and climate amelioration according to pollen data. Following the light layer accumulation with low productivity proxies was, most likely, associated with HE 1 cold climate condition at 16.2–15.2 ka BP, due to decreased nutrient supply by ECSCW water into the sea during the weaker summer Asian monsoon activity. During Bolling/Allerod warming, accompanied by

vegetation amelioration, sea-level rise induced further strengthening of Pacific water inflow, ventilation of deep water as well as increase in productivity. Stronger intensification in the East Asian summer monsoon at the beginning of Holocene 11.4 ka BP, transmits additional nutrients to the Sea, leading to growth of productivity and the formation of DL 1.

According to obtained IRD results, glacial condition in the northern Japan (East) Sea has undergone strong influence of the sea ice, although ice cover was not perennial and preferentially melted during summer seasons. Strong IRD peak during and after DL 10 was probably connected with long lasting DOI 8 warming, intensification of regional sea ice melting and IRD accumulation in summer seasons. The later IRD peak occurred during cold HE 1 following B/A warming. Siliceous phytoplankton production started simultaneously with a distinct decrease in sea ice influence at the end of B/A warming.

High resolution planktonic foraminifera $\delta^{18}O$ record from the Japan (East) Sea very sensible to inflow of the saline Pacific water, through the shallow Tsushima and Tsugaru Straits reveals useful evidences for global sea level reconstruction during the last 40 ka BP. The trend of $\delta^{18}O_{pf}$ changes in core LV 32–33 during 32 ka–15 ka BP resembles those of $\delta^{18}O$ records of planktonic and benthic foraminifera from the Red Sea, benthic $\delta^{18}O$ records from the North Atlantic, sea-level estimates from U–Th and ^{14}C dated corals and other dated evidences. Observed decrease in $\delta^{18}O_{pf}$ at 31–30 ka BP is likely to be related with abrupt sea level drop during the DL 5 formation. In the period of 29–24.5 ka BP, $\delta^{18}O_{pf}$ record indicates continuous decrease of sea level consistent with other observed sea level records except for an interruption of abrupt sea-level drop nearly at 27.5 ka BP. Then, $\delta^{18}O_{pf}$ data clearly indicates abrupt decrease of sea level coeval to cold event HE 2, followed by significant increase in $\delta^{18}O_{pf}$ signaling of fast sea-level rise coeval to GIS/CIS 2. According to $\delta^{18}O_{pf}$ changes, sea level declined considerably during 23–21.5 ka BP and was nearly constant at minimum standing during the LGM. Distinct increase in $\delta^{18}O_{pf}$ values since 18.6 ka BP which was consistent with coral results, indicates that the LGM low stand was abruptly terminated by a rapid sea-level rise of 10 to 15 m at about 19.0 ka BP. Final strong increase of $\delta^{18}O_{pf}$ was most probably associated with further sea-level rise, which occurred at 15.2–14.7 ka BP, close to the beginning of MWP-1A.

In general, the formation of DL layers in core LV 32–33 correlates well with regional and global climate changes on orbital and millennial time scales recorded in $\delta^{18}O$ values of the Greenland ice core, China cave stalagmites and global sea level changes over the last 40 ka BP (Fig. 5).

Acknowledgment

Many useful comments of two anonymous reviewers were greatly appreciated that helped strongly improve the manuscript. This research work was supported by the RFBR Project (13-05-00296a), K-Polar Program (PP13030) and Basic Research Program (PE14062) supported by KOPRI, Korea and the National Natural Science Foundation of China (40710069004, 41076038).

References

Arz, W., Lamy, F., Ganopolski, N., Nowaczyk, J., Patzold, J., 2007. Dominant Northern Hemisphere climate control over millennial-scale glacial sea-level variability. Quat. Sci. Rev. 26, 312–321.

Bard, E., Hamelin, B., Fairbanks, R.G., 1990. U/Th ages obtained by mass spectrometry in corals from Barbados: sea level during the past 130,000 years. Nature 346, 456–458.

Bard, E., Hamelin, B., Arnold, M., Montaggioni, L., Cabioch, G., Faure, G., Rougerie, F., 1996. Deglacial sea-level record from Tahiti corals and timing of the global meltwater discharge. Nature 382, 241–244.

Bauch, D., Erlenkeuser, H., Winckler, G., Pavlova, G., Thiede, J., 2002. Carbon isotopes and habitat of polar planktonic foraminifera in the Okhotsk Sea: the 'carbonate ion effect' under natural conditions. Mar. Micropaleontol. 45, 83–99.

Bemis, B.E., Spero, H.J., Bijma, J., Lea, D.W., 1998. Reevaluation of the oxygen isotopic composition of the planktonic foraminifera: experimental results and revised paleotemperature equations. Paleoceanography 13, 150–160.

Bond, G., Showers, W., Cheseby, M., Lotti, R., Almasi, P., deMenocal, P., Priore, P., Cullen, H., Hajdas, I., Bonani, G., 1997. A pervasive millennial-scale cycle in North Atlantic Holocene and glacial climates. Science 278, 1257–1266.

Chappell, J., 2002. Sea level changes forced ice breakouts in the Last Glacial cycle: new results from coral terraces. Quat. Sci. Rev. 21, 1229–1240.

Chapin, F.S., Starfield, A.M., 1997. The lags and novel ecosystems in response to transient climatic changes in Arctic Alaska. Clim. Chang. 35, 449–461.

Clark, P., McCabe, M., Mix, A., Weaver, A., 2004. Rapid rise of sea level 19,000 years ago and its global implications. Science 304, 1141–1144.

Conolly, J., Ewing, M., 1970. Ice-rafted detritus in Northwest Pacific deep-sea sediments. Geol. Soc. Am. Bull. 126, 219–231.

Cutler, K.B., Edwards, R.L., Taylor, F.W., Cheng, H., Adkins, J., Gallup, C.D., Cutler, P.M., Burr, G.S., Bloom, A.L., 2003. Rapid sea-level fall and deep-ocean temperature change since the last interglacial period. Earth Planet. Sci. Lett. 206, 253–271.

Dansgaard, W., Johnson, S.J., Claussen, H.B., Dahl-Jensen, D., Gundestrup, N.S., Hammer, C.U., Hvidberg, C.S., Steffensen, D., Sveinbjornsdottir, A.E., Jouzel, J., Bond, G., 1993. Evidence of general instability of past climate from a 250 kyr ice-core record. Nature 364, 218–220.

De Deckker, P., Yokoyama, Y., 2009. Micropalaeontological evidence for Late Quaternary sea-level changes in Bonaparte Gulf, Australia. Glob. Planet. Chang. 66, 85–92.

Duplessy, J.C., Labeyrie, L., Waelbroeck, C., 2002. Constraints on the ocean oxygen isotopic enrichment between the Last Glacial Maximum and the Holocene: paleoceanographic implications. Quat. Sci. Rev. 21, 315–330.

Epstein, S., Buchsbaum, R., Lowenstam, H.A., Urey, H.C., 1953. Revised oxygen-water temperature scale. Geol. Soc. Am. Bull. 64, 1315–1325.

Fairbanks, R.G., 1989. A 17000-year glacio-eustatic sea level record: influence of glacial melting rates on the Younger Dryas event and deep-ocean circulation. Nature 342, 637–642.

Gamo, T., Nozaki, Y., Sakai, H., Nakai, T., Tsubota, H., 1986. Spatial and temporal variations of water characteristics in the Japan Sea bottom water. J. Mar. Res. 44, 781–793.

Gorbarenko, S.A., 1983. Paleogeographic conditions in the central part of the Sea of Japan during Holocene and Late Pleistocene from data on $^{18}O/^{16}O$ in foraminifera tests. Okeanologia 23, 306–308 (in Russian with English abstract).

Gorbarenko, S.A., 1993. Reasons of the freshening of the surface water of the Japan Sea during last glaciation according $\delta^{18}O$ of the planktonic foraminifera. Okeanologia 33, 422–428 (in Russian with English abstract).

Gorbarenko, S.A., Chekhovskaya, M.P., Southon, J.R., 1998. Detailed environmental changes of the Okhotsk Sea central part during last glaciation-Holocene. Oceanologiya 38, 305–308 (in Russian with English abstract).

Gorbarenko, S.A., Southon, J.R., 2000. Detailed Japan/East Sea paleoceanography during the last 25 kyr: constrain from AMS dating and $d^{18}O$ planktonic foraminifera. Palaeogeogr. Palaeoclimatol. Palaeoecol. 156, 177–193.

Gorbarenko, S.A., Southon, J.R., Keigwin, L.D., Cherepanova, M.V., Gvozdeva, I.G., 2004. Late Pleistocene–Holocene oceanographic variability in the Okhotsk Sea: geochemical, lithological and paleontological evidences. Palaeogeogr. Palaeoclimatol. Palaeoecol. 209, 281–301.

Gorbarenko, S.A., Artemova, A.V., Goldberg, E.L., Vasilenko, Y.P., 2014. The response of the Okhotsk Sea environment to the orbital-millennium global climate changes during the Last Glacial Maximum, deglaciation and Holocene. Glob. Planet. Chang. 116, 76–90.

Gydrometeorologiya, gydrochimija morej. V. VIII, 2003. Japan Sea, Issue 1. In: Tersiev, F.C. (Ed.), Gydrometeoizdat, Sankt-Petersburg (398 pp (in Russian)).

Hanebuth, T., Stattegger, K., Grootes, P.M., 2000. Rapid flooding of the Sunda Shelf: a late-glacial sea-level record. Science 288, 1033–1035.

Harris, P., Zhao, G., Rosell-Mele, M., Tiedemann, R., Sarnthein, M., Maxell, J.R., 1996. Chlorine accumulation rate as a proxy for Quaternary marine primary productivity. Nature 383, 63–66.

Heinrich, H., 1988. Origin and consequences of cyclic ice rafted in the Northeast Atlantic Ocean during the past 130000 years. Quat. Res. 29, 142–152.

Heusser, L.E., Morley, J.J., 1985. Pollen and radiolarians records from deep-sea core RC14-103: climatic reconstructions of northeast Japan and northwest Pacific for the last 90,000 years. Quat. Res. 24, 60–72.

Igarashi, K., Yamamoto, M., Ikehara, K., 2011. Climate and vegetation in Hokkaido, northern Japan, since the LGM: pollen records from core GH02–1033 off Tokachi in the northwestern Pacific. J. Asian Earth Sci. 40, 1102–1110.

Ikehara, K., 2003. Late Quaternary seasonal sea-ice history of the Northeastern Japan Sea. J. Oceanogr. 59, 585–593.

Ikehara, K., Itaki, T., 2007. Millennial-scale fluctuations in seasonal sea-ice and deep-water formation in the Japan Sea during the late Quaternary. Palaeogeogr. Palaeoclimatol. Palaeoecol. 247, 131–143.

Itaki, T., Ikehara, K., Motoyama, I., Hasegawa, S., 2004. Abrupt ventilation changes in the Japan Sea over the last 30 ky: evidence from deep-dwelling radiolarians. Palaeogeogr. Palaeoclimatol. Palaeoecol. 208, 263–278.

Kawahata, H., Ohshima, H., Kuroyanagi, A., 2011. Ocean environmental change in the northwestern Pacific from the glacial times to Holocene. J. Asian Earth Sci. 40, 1189–1202.

Keigwin, L.D., 1998. Glacial-age hydrology of the far northwest Pacific ocean. Paleoceanography 13, 323–339.

Kiefer, T., Sarnthein, M., Erlenkeuser, H., Grootes, P., Roberts, A., 2001. North Pacific response to millennial-scale changes in ocean circulation over the last 60 ky. Paleoceanography 16, 179–189.

Kim, J.-M., Kennett, J., Park, B.-K., Kim, D.C., Kim, G.Y., Roark, B., 2000. Paleoceanographic changes during the last deglaciation, east Sea of Korea. Paleoceanography 15, 254–266.

Kroopnick, P.M., 1985. The distribution of the ^{13}C of total CO_2 in the world oceans. Deep-Sea Res. 32, 57–84.

Lavrenko, E.M., 1964. Physical Geographical Atlas of the World. Academy of Sciences of the USSR, Moscow (287 pp; (in Russian)).
Martin, S., Munoz, E., Drucker, R., 1992. The effect of severe storms on the ice cover of the northern Tatarsky Strait. J. Geophys. Res. 97 (17), 753–764.
Matsui, H., Tada, R., Oba, T., 1998. Low-salinity event in response to eustatic sea-level drop during the LGM: reconstruction based on salinity-balance model. Quat. Res. 37, 221–233 (in Japanese with English abstract).
Matsumoto, K., Yokoyama, Y., 2013. Atmospheric $\Delta^{14}C$ reduction in simulations of Atlantic overturning circulation shutdown. Glob. Biogeochem. Cycles 27. http://dx.doi.org/10.1002/gbc.20035.
Mortlock, R.A., Froelich, N.F., 1989. A simple method for the rapid determination of biogenic opal in pelagic marine sediments. Deep-Sea Res. 36, 1415–1426.
North Greenland Ice Core Project members, 2004. High-resolution record of Northern Hemisphere climate extending into the last interglacial period. Nature 431, 147–151.
Oba, T., Katon, M., Kitazato, H., Koizume, I., Omura, A., Sakai, T., Takayama, T., 1991. Paleoenvironmental changes in the Japan Sea during the last 85000 years. Paleoceanography 6, 499–518.
Oba, T., Murayama, M., Matsumoto, E., Nakamura, T., 1995. AMS C^{14} ages of Japan Sea cores from the Oki Ridge. Quat. Res. 34, 289–296 (in Japanese with English abstract).
Reimer, P.J., Bard, E., Bayliss, A., et al., 2013. Intcal 13 and Marine 13 radiocarbon age calibration curves 0–50,000 years cal BP. Radiocarbon 55, 1869–1887.
Sakamoto, T., Ikehara, M., Aoki, K., Jijima, K., Kimura, N., Nakatsuka, T., Wakatsuchi, M., 2005. Ice-rafted debris (IRD)-based sea-ice expansion events during the past 100 kyrs in the Okhotsk Sea. Deep-Sea Res. 52, 2275–2301.
Shackleton, N.J., Hall, M.A., Vincent, E., 2000. Phase relationships between millennial-scale events 64,000–24,000 years ago. Paleoceanography 15, 565–569.
Shackleton, N.J., Fairbanks, R.G., Chiu, T.-C., Parrenin, F., 2004. Absolute calibration of the Greenland time scale: implications for Antarctic time scales and for $\Delta^{14}C$. Quat. Sci. Rev. 23, 1513–1522.
Siddall, M., Rohling, E.J., Arnold-Labin, A., Hemleben, Ch., Meischner, D., Schmetzer, I., Smeed, D.A., 2003. Sea-level fluctuations during the last glacial cycle. Nature 423, 853–858.
Sladkov, A.N., 1967. Introduction in Pollen Analysis. Nauka Publications.
Stuiver, M., Reimer, P.J., 1993. Extended ^{14}C database and revised Calib3.0 ^{14}C age calibration program. Radiocarbon 35, 215–230.
Suk, M.S., Hong, G.H., Chung, C.S., Nam, S.Y., Kang, D.J., 1996. Distribution and transport of suspended particulate matter, dissolved oxygen and plant major inorganic nutrients in the Cheju Strait. J. Korean Soc. Oceanogr. 31, 55–63.
Tada, R., Koizumi, I., Cramp, A., Rahman, A., 1992. Correlation of dark and light layers, and the origin of their cyclicity in the Quaternary sediments from the Japan Sea. In: Pisciotto, K.A., Ingle Jr., J.C., Von Bareymann, M.T., Barron, J., et al. (Eds.), Proceedings of ODP, Scientific Results, 127/128, Part 1. College Station, Texas, pp. 577–601 (Ocean Drilling Program).
Tada, R., Irino, T., Koizumi, I., 1999. Land-ocean linkages over orbital and millennial timescales cycles recorded in late Quaternary sediments of the Japan Sea. Paleoceanography 14, 236–247.
Voelker, A.H., workshop participants, 2002. Global distribution of centennial-scale records for marine isotope stage (MIS) 3: a database. Quat. Sci. Rev. 21, 1185–1214.
Waelbroeck, C., Labeyrie, L., Michel, E., Duplessy, J.C., McManus, J.F., Lambeck, K., Balbon, E., Labracherie, M., 2002. Sea-level and deep water temperature changes derived from benthic foraminifera isotope records. Quat. Sci. Rev. 21, 295–305.
Wang, Y.J., Cheng, H., Edwards, R.L., An, Z.S., Wu, J.Y., Shen, C.C., Dorale, J.A., 2001. A high-resolution absolute-dated late Pleistocene monsoon records from Hulu Cave, China. Science 294, 2345–2348.
Wang, Y.J., Cheng, H., Edwards, R.L., Kong, X.G., Shao, X.H., Chen, S.T., Wu, J.Y., Jiang, X.Y., Wang, X.F., An, Z.S., 2008. Millennial- and orbital-scale changes in the East Asian monsoon over the past 224000 years. Nature 451, 1090–1093.
Watanabe, S., Tada, R., Ikehara, K., Fujine, K., Kido, Y., 2007. Changes in the bottom water oxygenation condition and possible causes of dark layers deposition in the Japan Sea during the last 160 kyrs. Palaeogeogr. Palaeoclimatol. Palaeoecol. 247, 50–64.
Wolff, E.W., Chappellaz, J., Blunier, T., Rasmussen, S.O., Svensson, A., 2010. Millennial-scale variability during the last glacial: the ice core record. Quat. Sci. Rev. 29, 2828–2838.
Yakynin, L.P., 1979. Sea ice investigation of the Far Eastern Seas. Proc. Far East. Sci. Res. Hydro Meteorol. Inst. 77, 102–107 (in Russian).
Yarichin, V.G., 1980. Steady state of the Japan Sea circulation. In: Pokudov, V. (Ed.), Problems of Oceanography. Hydrometeoizdat, Leningrad, pp. 46–61 (in Russian).
Yokoyama, Y., Lambeck, K., De Deckker, P.P.J., Fifield, L.K., 2000. Timing of the last glacial maximum from observed sea-level minima. Nature 406, 713–716.
Yokoyama, Y., Deckker, De, Lambeck, K., Fifield, L.K., 2001. Sea-level at the Last Glacial Maximum: evidence from northwestern Australia to constrain ice volumes for oxygen isotope 2. Palaeogeogr. Palaeoclimatol. Palaeoecol. 165, 281–297.
Yokoyama, Y., Naruse, T.N., Ogawa, O., Tada, R., Kitazato, H., Ohkouchi, N., 2006. Dust influx reconstruction during the last 26,000 years inferred from a sedimentary leaf wax record from the Japan Sea. Glob. Planet. Chang. 54, 239–250.
Yokoyama, Y., Kido, Y., Tada, R., Minami, I., Finke, R.C., Hiroyuki, M., 2007. Japan/East Sea oxygen isotope stratigraphy and global sea-level changes for the last 50,000 years recorded in sediment cores from the Oki Ridge. Palaeogeogr. Palaeoclimatol. Palaeoecol. 247, 5–17.
Yokoyama, Y., Esat, T.M., 2011. Global climate and sea level: enduring variability and rapid fluctuations over the past 150,000 years. Oceanography 24, 54–69. http://dx.doi.org/10.5670/oceanog.2011.27.
Yoon, J.-H., Kim, Y.-J., 2009. Review on the seasonal variation of the surface circulation in the Japan/East Sea. J. Mar. Syst. 78, 226–236. http://dx.doi.org/10.1016/j.jmarsys.2009.03.003.